GLIA

GLIA 58:1847–1857 (2010)

Tubulin Polymerization Promoting Protein (TPPP/p25) as a Marker for Oligodendroglial Changes in Multiple Sclerosis

ROMANA HÖFTBERGER,[1] STEPHANIE FINK,[1] FAHMY ABOUL-ENEIN,[2] GERGÖ BOTOND,[1] JUDIT OLAH,[3] TIMEA BERKI,[4] JUDIT OVADI,[2] HANS LASSMANN,[5] HERBERT BUDKA,[1] AND GABOR G. KOVACS[1]*

[1]*Institute of Neurology, Medical University of Vienna, Vienna, Austria*
[2]*Department of Neurology, SMZ-Ost Donauspital, Vienna, Austria*
[3]*Institute of Enzymology, Biological Research Center, Hungarian Academy of Sciences, Budapest, Hungary*
[4]*Faculty of Medicine, Department of Immunology and Biotechnology, University of Pécs, Hungary*
[5]*Department of Neuroimmunology, Center for Brain Research, Medical University of Vienna, Vienna, Austria*

KEY WORDS
degeneration; multiple sclerosis; oligodendrocyte; remyelination; tubulin polymerization promoting protein (TPPP/p25)

ABSTRACT
Multiple sclerosis (MS) is an idiopathic chronic inflammatory demyelinating disease of the central nervous system with variable extent of remyelination. Remyelination originates from oligodendrocyte (OG) precursor cells, which migrate and differentiate into mature OG. Tubulin polymerization promoting protein (TPPP/p25) is located in mature OG and aggregates in oligodendroglial cytoplasmic inclusions in multiple system atrophy. We developed a novel monoclonal anti-TPPP/p25 antibody to quantify OG in different subtypes and disease stages of MS, and possible degenerative changes in OG. We evaluated autopsy material from 25 MS cases, including acute, primary progressive, secondary progressive, relapsing remitting MS, and five controls. Demyelinated lesions revealed loss of TPPP/p25-positive OG within the plaques. In remyelination, TPPP/p25 was first expressed in OG cytoplasms and later became positive in myelin sheaths. We observed increased numbers of TPPP/p25 immunoreactive OG in the normal appearing white matter (NAWM) in MS patients. In MS cases, the cytoplasmic area of TPPP/p25 immunoreactivity in the OG was higher in the periplaque area when compared with NAWM and the plaque, and TPPP/p25 immunoreactive OG cytoplasmic area inversely correlated with the disease duration. There was a lack of phospho-TDP-43, phospho-tau, α-synuclein, and ubiquitin immunoreactivity in OG with enlarged cytoplasm. Our data suggest impaired differentiation, migration, and activation capacity of OG in later disease stages of MS. Upregulation of TPPP/p25 in the periplaque white matter OG without evidence for inclusion body formation might reflect an activation state. Distinct and increased expression of TPPP/p25 in MS renders it a potential prognostic and diagnostic marker of MS.

INTRODUCTION

Multiple sclerosis (MS) is a chronic inflammatory and demyelinating disease of the central nervous system (CNS) of unknown origin. Underlying pathogenetic mechanisms are supposed to be heterogeneous and complex (Lassmann et al., 2007). In MS, demyelinating lesions with relatively preserved axons may occur in the entire CNS with predilection of the optic nerves, the periventricular and subcortical white matter, the cerebellum, and the spinal cord (Lassmann et al., 2007). Self-repair mechanisms in MS include remyelination with variable extent (Blakemore, 1974; Prineas et al., 1993). Why remyelination differs between patients, and commonly declines with age and disease duration, remains unsolved (Goldschmidt et al., 2009; Patrikios et al., 2006).

Remyelination originates from a pool of oligodendrocyte precursor cells (OPC), which reside throughout the entire grey and white matter of the CNS and in the subventricular zone (Dubois-Dalcq et al., 2008), and are able to migrate and differentiate into mature oligodendrocytes (OG) (Di Bello et al., 1999). Whereas remyelination in early MS is highly efficient (Prineas et al., 1989; Raine and Wu, 1993), the density of OPC in chronic inactive lesions is significantly reduced (Wolswijk, 2000). Possible mechanisms include a depletion of the OPC pool due to repeated de- and remyelination processes (Keirstead et al., 1998), impaired differentiation and migration of precursor cells into lesion areas (Kuhlmann et al., 2008), or due to a disturbed microenvironment within the lesions (Chang et al., 2002). Recently, α-synuclein, a protein, which is involved in some neurodegenerative diseases including Parkinson's disease and multiple system atrophy (MSA), was found expressed in OG in actively demyelinating MS lesions suggesting response to increased cellular oxidative stress and OG degeneration in MS (Lu et al., 2009).

Grant sponsor: EU Grant FP6; Grant numbers: BNEII No LSHM-CT-2004-503039 and EU FP6-2004-LIFESCIHEALTH-I; Grant sponsor: Hungarian National Scientific Research Fund; Grant numbers: OTKA T-067963 and PD 76793; Grant sponsors: BioSim and Janos Bolyai Research Scholarship of the Hungarian Academy of Sciences.

*Correspondence to: Gabor G. Kovacs, Institute of Neurology, AKH 4J, Währinger Gürtel 18-20, POB 48, A-1097 Vienna, Austria.
E-mail: gabor.kovacs@meduniwien.ac.at

Received 28 October 2009; Accepted 29 June 2010

DOI 10.1002/glia.21054

Published online 24 August 2010 in Wiley Online Library (wileyonlinelibrary.com).

Tubulin polymerization promoting protein (TPPP/p25) shows high affinity for the microtubular system, and in the CNS, it is selectively expressed by OG (Hlavanda et al., 2002; Kovacs et al., 2004; Lehotzky et al., 2004). In the developing rat brain, TPPP/p25 co-localizes with markers for myelinating OG (2′3′-cyclic nucleotide 3′phosphodiesterase, CNP), but not with those for OPC (NG2) or premyelinating OG (CD9), confirming that TPPP/p25 is specifically expressed in mature OG (Skjoerringe et al., 2006). TPPP/p25 is supposed to be involved in the rearrangement of the microtubule system during the process elongation prior to myelin formation, which plays an important role in myelination in the developing brain and renewal in the adult brain (Kovacs et al., 2004; Lehotzky et al., 2010; Skjoerringe et al., 2006). In contrast to myelin basic protein (MBP), proteolipid protein (PLP), and CNP, the antibody for TPPP/p25 strongly labels the OG cell bodies and only to lesser extent myelin sheaths, which makes a reliable quantification of mature OG possible. As TPPP/p25 has been found co-localized with α-synuclein in cytoplasmic inclusions of OG in MSA, TPPP/p25 may allow to identify degenerative changes in OG (Kovacs et al., 2004).

Using a novel monoclonal anti-TPPP/p25 antibody, we investigated mature OG in different subtypes and disease stages of MS and examined whether pathological changes suggestive for primary (neuro-) degenerative CNS disease may be found, or not.

MATERIALS AND METHODS

Production of Mouse Monoclonal Antibody 6C10 Against TPPP/p25

Female Balb/c mice (6 weeks old, Charles River) were immunized into each hind footpad, and intraperitoneally (i.p.) with 30 μg of TPPP/p25 peptide dissolved in CFA (complete Freund adjuvant), followed with two i.p. boosts in incomplete Freund adjuvant 21 and 14 days later. The splenocytes of the animal with best response were fused to Sp-2/0 Ag14 mouse myeloma cells (originally obtained from Flow Laboratories UK and maintained in our cell depository) according to the method described (Kohler and Milstein, 1975). Supernatants were assayed for the presence of anti-TPPP/p25 antibodies using an indirect simple binding enzyme-linked immunosorbent assay (ELISA). The positive wells were cloned and further characterized.

For ELISA, the microtiter plate was coated with 5 μg/mL (100 μL/well) human recombinant TPPP/p25 in phosphate buffered saline (PBS) overnight at 4°C. The wells were blocked with 0.1% bovine serum albumin (BSA) in PBS for 1 h at room temperature. Next, the plate was incubated with serial dilutions of the monoclonal anti-TPPP/p25 antibody (anti-TPPP/p25 mAB) in the concentration range between 5 and 0.05 μg/mL for 1 h at room temperature. Then, the plate was incubated with the anti-mouse IgG-peroxidase conjugate (dilution 1:5,000). Both antibodies were in PBS buffer containing 0.1% BSA, and incubated for 1 h at room temperature. Between each incubation steps, the wells were washed three times with PBS containing 0.05% Tween20. o-Phenylenediamine in the concentration of 3.7 mM with 0.03% peroxide was used as substrate solution. The peroxidase-catalyzed reaction was stopped after 10 min with 1 M H_2SO_4; absorbance was read at 490 nm with a Wallace Victor 2 multiplate reader.

The protein samples were separated by 12% sodium dodecyl sulfate polyacrylamide gel electrophoresis and blotted on Immobilon-P polyvinylidene fluoride (PVDF) membrane (Millipore). To test the specificity of the anti-TPPP/p25 mAb, membrane with human recombinant TPPP/p25, its two homologues and brain extracts was incubated with 0.2 μg/mL IgG anti-TPPP/p25 mAb and then with goat anti-mouse IgG-peroxidase conjugate (1:10,000, Sigma-Aldrich). Enhanced chemiluminescence Western Blotting Detection reagents (Amersham Biosciences) and Kodak X-Omat AR film were used for visualization and the program ImageJ (1.37v) for densitometry. The cytosolic brain extract was prepared as described previously (Olah et al., 2006). The protein concentration was determined by the Bradford method using the Bio-Rad protein assay kit (Bradford, 1976).

Specificity of TPPP/p25 Antibody for Immunohistochemistry

To test the specificity of the anti-TPPP/p25 antibody for immunohistochemistry, we applied different dilutions and antigen retrieval methods using paraffin-embedded brain tissue samples from one case with temporal epilepsy (temporal cortex and white matter), one with MSA (pons), one with Parkinson's disease (mesencephalon), and one autopsy case without neurological disease (frontal cortex). For further antibody specification, we used electron microscopy. After incubation of the paraffin-embedded tissue sections with anti-TPPP/p25 mAB, we applied ultra-small gold conjugated secondary antibody followed by silver-enhancing method. Slides were mounted with resin and examined in light microscopy. Areas with immunoreactive cells were reembedded for ultrasectioning. We used a Zeiss electron microscopy to evaluate the sections.

Cases

We used formalin-fixed paraffin-embedded archival human autopsy material of acute MS (AMS) cases of Marburg's type (AMS; $n = 4$; age range, 28–40 years; median, 34 years; disease duration, 6 ± 2 months), primary progressive MS cases (PPMS; $n = 5$; age range, 30–64 years; median, 34 years; disease duration, 35 ± 79 months), secondary progressive MS cases ($n = 5$; age range, 38–65 years; median, 40 years; disease duration, 156 ± 193 months), relapsing remitting MS cases (RRMS; $n = 11$; age range, 24–84 years; median, 59 years; disease duration, 216 ± 148 months), and age matched controls ($n = 5$; age range, 27–81 years; me-

dian, 35 years). Clinical categorization of MS subtypes was made according to McDonalds criteria (McDonald et al., 2001). Control patients without any evidence for neurological disease died due to cardiorespiratory failure. The Ethics Committee of the Medical University of Vienna approved the study.

Immunohistochemistry

The following well-characterized primary antibodies were used: monoclonal (mouse) antibodies: anti-CNP (1:1,000; Sternberger Monoclonals Incorporated, Lutherville, MD), anti-PLP (1:1,000; Serotec, Oxford, UK), anti-CD3 (1:100; Dako, Glostrup, Denmark), anti-CD8 (1:100; Dako), anti-CD20 (1:200; Dako), anti-CD45R0 (1:100; Dako), anti-CD68 (1:1,000; Dako), anti-phosphorylated neurofilament protein (1:5,000; SMI-31, Sternberger Monoclonals), anti-TPPP/p25 (1:2,000; see above), anti-tau AT8 (1:200, Pierce Biotechnology, Rockford, IL), anti-4R tau (RD4, 1:200, Upstate, Charlottesville, VA), anti-3R tau (RD3, 1:2,000, Upstate), anti-phospho-TDP-43 (pS409/410, 1:2,000, Cosmo Bio Co., Tokyo, Japan), anti-TDP-43 (1:2,000, Abnova Corp. Taipei, Taiwan), anti-HLA-DR (1:100, Dako), and anti-α-synuclein (1:10,000, clone 4D6, Signet, Dedham, MA), anti-MRP14 (1:100; BMA Biomedicals, Augst, Switzerland); polyclonal antibodies*:* anti-TPPP/p25 [rat, 1:1,000; (Kovacs et al., 2007)], anti-MBP (rabbit, 1:200; Dako), anti-p62 (guinea pig, 1:4,000, Progen Biotechnik GmBh, Heidelberg, Germany), and anti-glial fibrillary acidic protein (rabbit, 1:3,000, Dako).

After deparaffinization and incubation in 3% hydrogen peroxide in methanol to block endogenous peroxidase activity, sections were incubated with primary antibodies. The DAKO EnVision© detection kit, peroxidase/DAB, rabbit/mouse (Dako, Glostrup, Denmark) was used for visualization of the antibody reaction (Hoftberger et al., 2007).

Fluorescence Double Immunolabeling

Fluorescence labeling was performed as described in detail previously (Hoftberger et al., 2004). The following well-characterized fluorescent secondary antibodies were used: Alexa Fluor-488 coupled goat anti-rabbit IgG (Molecular Probes, Eugene, OR), Alexa Fluor-488 coupled goat anti-mouse IgG (Molecular Probes, Eugene, OR), Cy3 coupled donkey anti-mouse IgG (Jackson Immuno Research Laboratories, West Grove, PA), and Cy3 coupled streptavidin (Jackson ImmunoResearch). Appropriate combinations of primary and fluorescent secondary antibodies were used. The slides were analyzed with a Zeiss LSM 510 motorized confocal laser scan microscope (Carl Zeiss, Jena, Germany) equipped with an argon-ion laser source (488 nm excitation) and two helium neon lasers (543 and 633 nm excitation). To eliminate "bleed-through" from either channel, an appropriate combination of excitation and barrier filters (bandpass filter 505–530 nm and longpass filters 560 nm) was used.

Classification of Lesional Activity

As described previously (Bruck et al., 1995), presence of MRP14 positive macrophages characterized early active lesions, and macrophages with myelin degradation products positive for major myelin proteins (MBP, PLP) characterized late active lesions. Inactive lesions either contained macrophages with empty vacuoles or were devoid of macrophages. Periplaque white matter (PPWM) was defined as a strip of tissue, extending 10 mm from the border of the active or inactive lesions into the surrounding normal white matter. The normal appearing white matter (NAWM) was defined as the white matter with a minimum of 2 cm distance to the PPWM. Remyelinated lesions were classified as areas with thin myelin sheets around axons (shadow plaques).

Quantitation of Immunolabeled Cells

The amount of TPPP/p25-expressing OG was evaluated in fields measuring 1 mm^2 in the MS plaques, PPWM, NAWM of MS cases, and anatomically matched normal white matter of control cases.

Quantitation of OG Cytoplasm

For the evaluation of the cytoplasmic size of TPPP/p25 immunoreactive OG made from digital microphotographs each covering an area of 85.000 μm^2 were made from plaques, PPWM, NAWM in MS, and NAWM in control cases. Only TPPP/p25 immunoreactive OG with visible nucleus were evaluated. First, TPPP/p25 immunoreactive OG were optically dissected and copied into a white background image. This was followed by optical dissection of the nucleus. The remaining cytoplasmic area was converted into black. To determine the density of black dots per unit of cytoplasmic area, we used analySIS software (Soft Imaging System, Münster, Germany) with equal threshold values. The area fraction of the black pixels represented the size of the cytoplasmic area and was used for statistical analysis. This procedure is illustrated in Figure 1A.

Statistical Analysis

One-way analysis of variance test with Bonferroni *post-hoc* test was used to compare the counts of TPPP/p25 immunoreactive OG (/mm^2) in the NAWM and to compare cytoplasmic areas of OG in different regions in controls and MS subtypes. Spearman correlation test was used to correlate mean values of OG areas in different regions of MS subtypes with age at death and duration of disease. All the tests were classified as significant if the P value was <0.05. All values are expressed as means ± standard error of the mean. SPSS Version X© standard software package was used (SPSS, Chicago, IL).

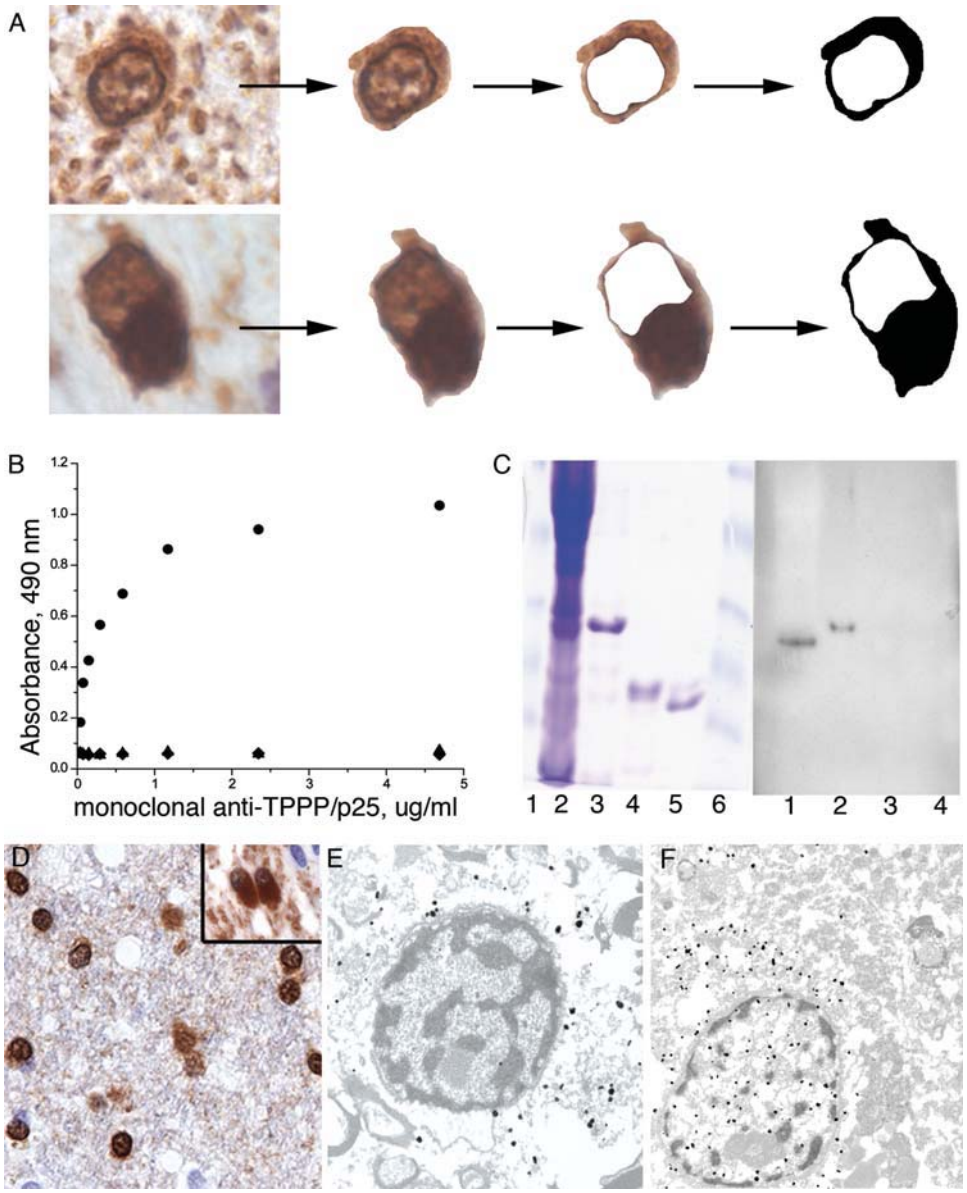

Fig. 1. **A**: Procedure for the evaluation of the cytoplasmic size of TPPP/p25 immunoreactive OG. First, immunoreactive OG were optically dissected and copied into a white background image. This was followed by optical dissection of the nucleus. The remaining cytoplasmic area was converted into black. The density of black dots was measured (see text for more details). **B**: Testing the specificity of the monoclonal anti-TPPP/p25 serum by enzyme-linked immunosorbent assay. The plate was coated with human recombinant TPPP/p25 (round dots), TPPP/p20 (triangle), or with TPPP/p18 (diamonds) and then incubated with serial dilutions of the monoclonal anti-TPPP/p25 serum. The data points are average of three parallel experiments. IC_{50} value of the serum: 0.15 μg/mL. **C**: Testing of the monoclonal anti-TPPP/p25 antibody. The panel on the left side demonstrates 13.5% sodium dodecyl sulfate polyacrylamide gel electrophoresis. Lane 1: molecular weight marker (85, 47, 36, 26, and 20 kDa); Lane 2: 35 μg bovine brain extract; Lane 3: 1 μg TPPP/p25; Lane 4: 1 μg TPPP/p20; Lane 5: 1 μg TPPP/p18; and Lane 6: molecular weight marker. The panel on the right side represents Western Blot. Lane 1: 35 μg bovine brain extract; Lane 2: 50 ng TPPP/p25; Lane 3: 50 ng TPPP/p20; and Lane 4: 50 ng TPPP/p18. **D**: Immunohistochemical staining for TPPP/p25 using the novel monoclonal antibody demonstrates immunopositivity in OG (temporal lobe white matter of a representative control brain; ×40). In the right upper inset, immunopositivity in Papp-Lantos bodies in a representative case of multiple system atrophy is demonstrated (pontine base; ×40). **E, F**: Representative electron microscopical images of OG demonstrating TPPP/p25 specific immunogold particles in the cytoplasm and nucleus. [Color figure can be viewed in the online issue, which is available at wileyonlinelibrary.com.]

RESULTS

Characterization of the Novel Monoclonal Anti-TPPP/p25 Antibody

The anti-TPPP/p25 mAb was tested by ELISA using human recombinant TPPP/p25 as antigen and also by Western blot using bovine brain cellular extract. The monoclonal anti-TPPP/p25 mAb showed high immunoreactivity against the human TPPP/p25 both by ELISA (Fig. 1B) and Western blot (Fig. 1C). No cross-reactivity was detected when the homologues of TPPP/p25 (TPPP/p20 and TPPP/p18) were used as antigens. The sequence comparison of the three proteins showed 53% identity. The pair wise comparisons of similarities are 81, 76, and 75% for TPPP/p25-TPPP/p20,

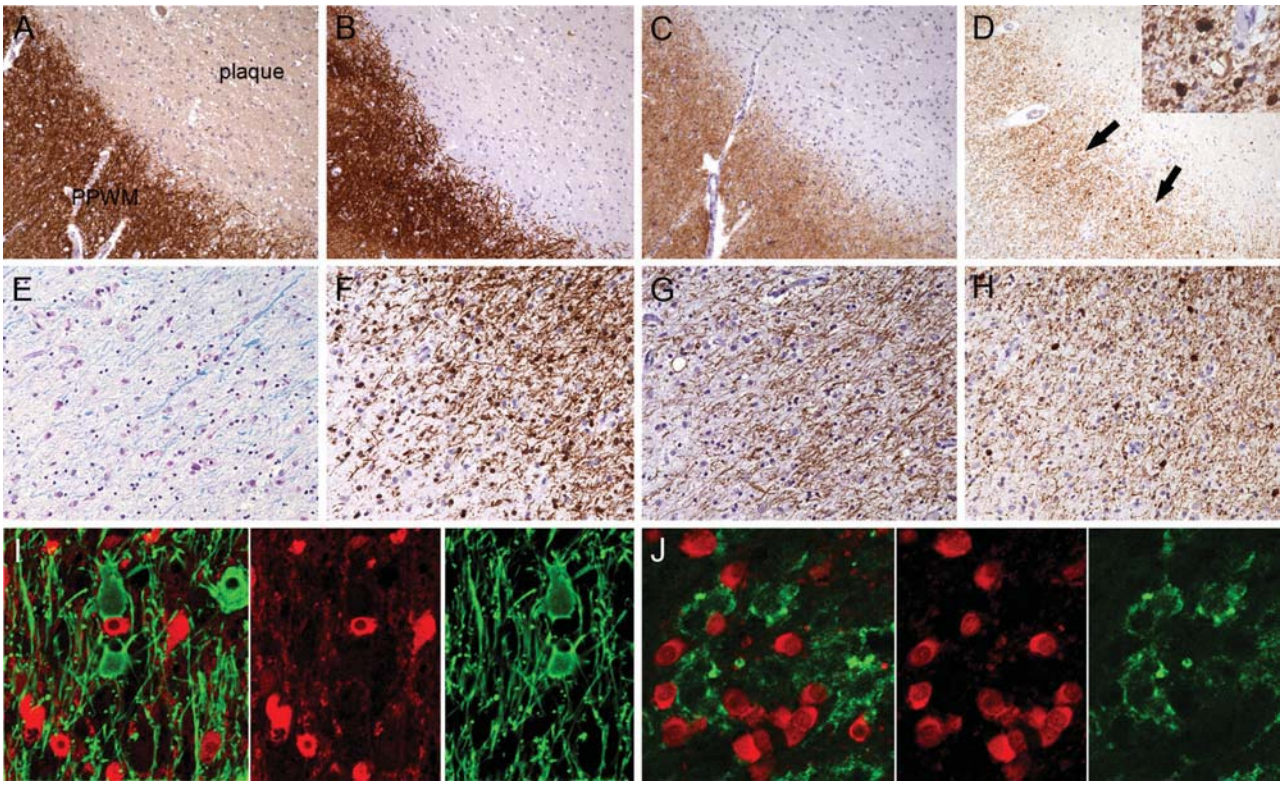

Fig. 2. Immunohistochemistry and confocal labeling of demyelinating and remyelinating lesions in multiple sclerosis. Areas with loss of MBP (**A**), PLP (**B**), and CNP (**C**) are also negative for TPPP/p25 (**D**). OG number is increased in the PPWM and show larger cytoplasms (D). Remyelinated areas feature thin and irregular myelin sheaths (**E**, LFB/PAS) and show strong immunopositivity for CNP (**F**), PLP (**G**), and TPPP/p25 (**H**). TPPP/p25 is not co-localized with astrocytes (**I**, TPPP/p25 red, GFAP green) or microglia/macrophages (**J**, TPPP/p25 red, HLA DR green). Original magnification: (A–D) ×100; (D, detail) ×600; (E–H) ×200; (I, J) ×630. [Color figure can be viewed in the online issue, which is available at wileyonlinelibrary.com.]

TPPP/p20-TPPP/p18, and TPPP/p25-TPPP/p18, respectively. TPPP/p25 was also observed in bovine brain extract ($\sim$ 3.5 ng TPPP/p25/mg protein). These data provided evidence that the antibody is highly specific for TPPP/p25.

For immunostaining, best results were obtained using epitope retrieval of 10 min citrate buffer (pH6) followed by formic acid (98%) treatment for 1 min. We observed immunoreactivity for TPPP/p25 in OG cell bodies and to lesser extent OG nuclei, myelin, and glial cytoplasmic inclusions in MSA with light and electron microscopy. TPPP/p25 most intensely stained the cytoplasm of mature OG (diffuse staining pattern) and intracytoplasmic inclusion bodies in degenerative OG in MSA, whereas myelin sheaths were only to a lesser extent positive (Fig. 1D–F). Neither in control brains nor in MS did we observe TPPP/p25 immunoreactivity in the neuronal cytoplasm.

Distribution of TPPP/p25 Positive OG in Demyelinating Lesions

Labeling of demyelinating MS lesions revealed a severe loss of TPPP/p25-positive OG within MS plaques. Those areas that showed a loss of MBP, PLP, and CNP were also negative for TPPP/p25 (Fig. 2A–D). Remyelinating areas were characterized by thin and irregular myelin sheaths as demonstrated in the Luxol fast blue-periodic acid Schiff (LFB/PAS) stain (Fig. 2E). These areas showed strong immunoreactivity for CNP, PLP, and TPPP/p25 (Fig. 2F–H). TPPP/p25 did not co-localize with markers for astrocytes or microglia/macrophages (Fig. 2I,J). In the course of remyelination, TPPP/p25 appeared first strongly expressed in the cytoplasm of OG together with CNP (Fig. 3A), and later on also in the myelin sheaths together with PLP and MBP (Fig. 3B,C).

Higher Number of TPPP/p25 Positive OG in the NAWM of MS

OG counts were evaluated in the anterior (level of caudate nucleus) and posterior (occipital) periventricular regions in different MS subtypes and controls (Table 1). In the NAWM, the number of TPPP/p25 positive OG were significantly higher in all MS patients (pooled) compared with controls (all MS 569.52 $\pm$ 59.97; controls 304.71 $\pm$ 55.46, $P < 0.01$) (Figs. 4A and 5A,B). Although all examined MS subtypes showed higher values compared with controls, comparisons of the subgroups with controls reached no statistical significance (Table 1, Fig. 4A).

Positive Correlation Between OG Counts in the PPWM and NAWM

OG counts in the PPWM, inactive plaques, and remyelinating areas, and corresponding NAWM were eval-

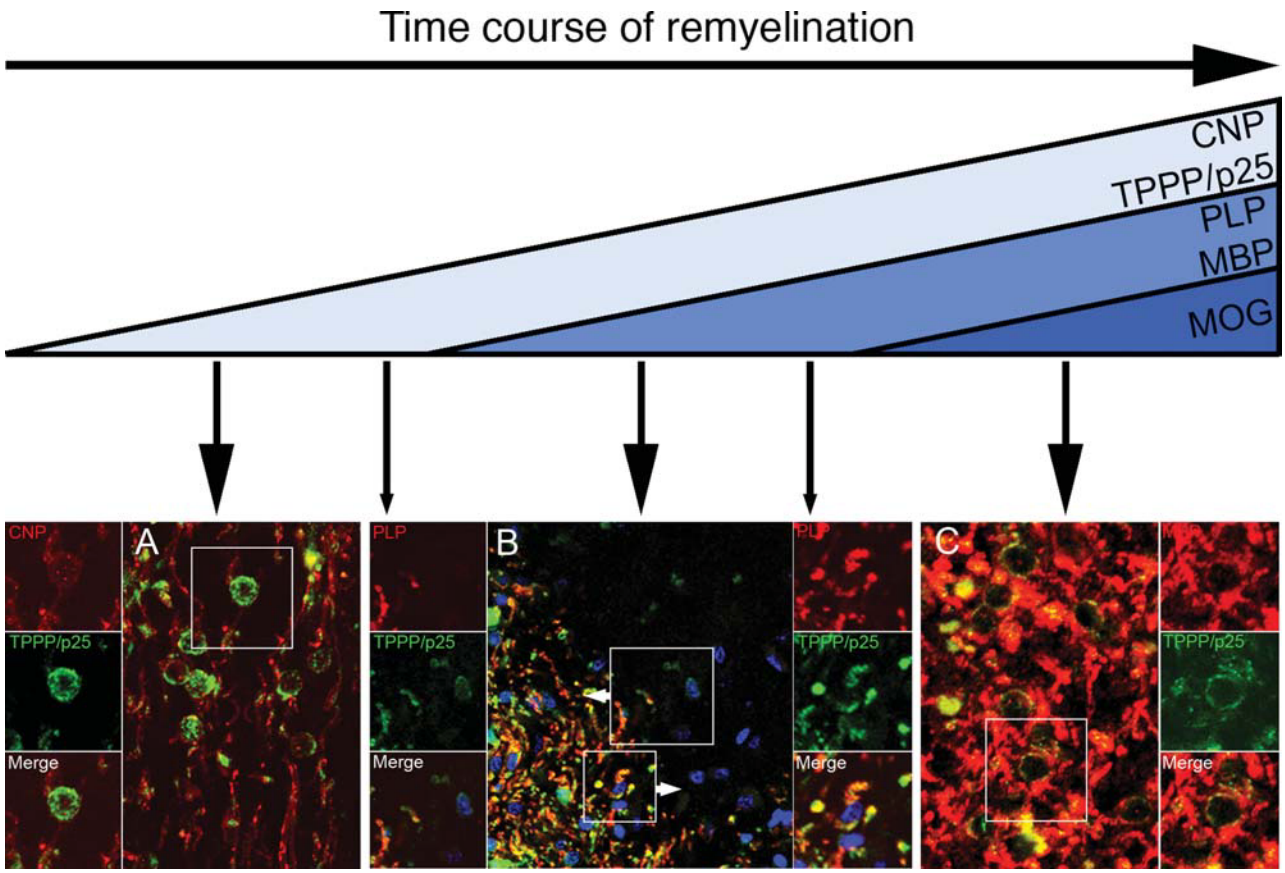

Fig. 3. Time course of remyelination: overview of expression of myelin-specific proteins. TPPP/p25 occurs very early in remyelination at the same time as CNP and is first strongly expressed in the cytoplasm (**A**, CNP red, TPPP/p25 green). Subsequently, TPPP/p25 is also found in myelin sheaths along with the myelin-specific proteins PLP (**B**, PLP red, TPPP/p25 green, Topro3, nuclei, blue) and MBP (**C**, MBP red, TPPP/p25 green). [Color figure can be viewed in the online issue, which is available at wileyonlinelibrary.com.]

uated in different anatomical regions (Table 1). The numbers of TPPP/p25 positive OG in the PPWM correlated significantly with OG numbers in the NAWM ($r = 0.70$, $P < 0.001$). No correlation was found between OG numbers in the inactive plaques versus NAWM ($r = 0.25$, $P < 0.19$), as well as between the remyelinating area and NAWM ($r = 0.31$, $P < 0.31$) (Fig. 4B). Only a trend was found for the correlation between the OG count in the PPWM and the remyelinating area ($r = 0.55$, $P < 0.07$) but not between PPWM versus inactive plaques ($r = 0.25$, $P < 0.19$).

Cytoplasmic TPPP/p25 Immunoreactivity Distinguishes Lesional Activity in MS

TPPP/p25 immunoreactive OG cytoplasmic area was evaluated in different lesions in MS subtypes (Table 1). In all MS, the area of TPPP/p25 immunoreactivity in the OG cytoplasm was significantly higher in the PPWM compared with the NAWM, the plaque (active as well as inactive lesions), and the white matter of controls ($P < 0.05$) (Figs. 4C and 5C–F).

When MS subtypes were evaluated separately, we observed a trend for higher values in the PPWM when compared with NAWM and plaque in all subtypes of MS. Bonferroni *post-hoc* correction indicated significant difference only in PPMS (PPWM vs. plaque: $P < 0.004$) and RRMS (PPWM vs. plaque and PPWM vs. NAWM, both $P < 0.001$).

TPPP/p25 immunoreactive OG cytoplasmic area in the NAWM of all MS inversely correlated with the disease duration ($r = -0.65$, $P < 0.002$) and age at death ($r = -0.433$, $P \leq 0.05$). Similarly, when the PPWM was evaluated, we observed an inverse correlation with disease duration ($r = -0.53$, $P < 0.01$) and age ($r = -0.524$, $P < 0.01$). TPPP/p25 immunoreactive OG cytoplasmic area in the plaque correlated inversely only with the disease duration ($r = -0.47$, $P < 0.02$), and there was a trend for correlation with age at death ($r = -0.33$, $P \leq 0.1$) (Fig. 4D).

Distribution of Phospho-Tau, α-Synuclein, and TDP-43 Immunoreactivity in MS

Demyelinated lesions, PPWM as well as NAWM were investigated for the expression of Gallyas-, phospho-Tau (AT8)-, 3R-tau, 4R-tau, α-synuclein-, p62-, TDP-43-, and phospho-TDP-43-immunopositivity. No inclusion-like

TABLE 1. Summary of Cases and Regions Evaluated for TPPP/p25 Oligodendrocyte (OG) Counts and Cytoplasmic Area

Group	No. of cases	F:M	Age ± SE (range)	Disease (mo) duration ± SE (range)
All cases: Clinical data				
Acute MS	4	2:2	34 ± 12 (26)	6 ± 2 (4)
SPMS	5	2:3	40 ± 13 (31)	156 ± 193 (492)
RRMS	11	8:3	59 ± 20 (60)	216 ± 148 (408)
PPMS	5	2:3	34 ± 15 (34)	35 ± 79 (192)
Control	5	3:2	35 ± 23 (54)	

Group	No. of cases	Anterior PV	Posterior PV	Sum of regions
OG count in NAWM: No. of evaluated regions				
Acute MS	4	5	0	5
SPMS	3	0	4	4
RRMS	4	3	2	5
PPMS	4	4	1	5
All MS	15	12	7	19
Control	5	10	4	14

Group	No. of cases	PPWM/NAWM	IA/NAWM	Remyelination/NAWM
OG count correlation between lesions: No. of evaluated lesions				
Acute MS	4	7	3	5
SPMS	5	7	7	0
RRMS	10	18	12	6
PPMS	5	7	5	1
All MS	24	39	27	12

Group	NAWM	PPWM	Plaque	Sum of regions
OG cytoplasmic area: No. of evaluated lesions				
Acute MS	4	4	4	12
SPMS	3	4	4	11
RRMS	9	9	9	27
PPMS	4	5	5	14
All MS	20	22	22	64
Control	5	0	0	5

NAWM, normal appearing white matter; PPWM, periplaque WM; PV, periventricular; PPMS, primary progressive MS; RRMS, relapsing remitting MS; SPMS, secondary progressive multiple sclerosis.

structures were visible with these stainings. Diffuse cytoplasmic immunoreactivity for α-synuclein was observed in some astrocytes, OG, microglia/macrophages, and axons in and around demyelinated plaques. Some MS subtypes showed OG degeneration with numerous apoptotic figures, which strongly labeled for TPPP/p25 (Fig. 5G). In a single MS case exhibiting particularly abundant apoptotic OG, dense immunostaining of TPPP/p25 was found in enlarged OG cytoplasms in the PPWM. However, these were not labeled with Gallyas stain, α-synuclein (Fig. 5H), p62, or ubiquitin immunostaining.

DISCUSSION

We developed and characterized a novel monoclonal antibody for TPPP/p25, a specific marker for OG and myelin. With this marker, we found that (1) the numbers of OG positive for TPPP/p25 were increased in the NAWM of MS patients; (2) OG counts in the NAWM correlated significantly with that in the PPWM; (3) The cytoplasmic area of TPPP/p25 immunopositivity in OG was significantly higher in the PPWM as in other lesions; (4) The cytoplasmic area of TPPP/p25 immunoreactivity correlated inversely with duration of illness in different lesions; (5) Apoptotic OG immunoreactive for TPPP/p25 were abundant in a subset of MS cases, however, (6) pathological changes such as cytoplasmic inclusion bodies or aggregations usually seen in primary (neuro-) degenerative CNS diseases were absent.

It has been demonstrated that tubulin/microtubule is the major target of TPPP/p25 protein (Hlavanda et al., 2002). These results support an essential role for TPPP/p25 in OG differentiation, likely via rearrangement of the microtubule system during the process elongation prior to the onset of myelination. This is reflected by the time course of remyelination, where TPPP/p25 occurs very early in OG differentiation together with CNP (Baumann and Pham-Dinh, 2001; Skjoerringe et al., 2006), shortly before expression of myelin-specific proteins such as PLP, MBP, or MOG (Baumann and Pham-Dinh, 2001; Chang et al., 2002; Lindner et al., 2008) (Fig. 3). Overall, the proper upregulation of TPPP/p25 protein level during differentiation may be essential for the dynamics of cytoskeletal rearrangement through its binding to microtubules, which are integral to the structural stability and plasticity of the OG cytoskeleton (Lehotzky et al., 2010). While TPPP/p25 mRNA was found in OG and neurons but not in astrocytes, post-transcriptional regulation induces TPPP/p25 protein expression specifically in OG in nonpathological conditions (Cahoy et al., 2008; Lehotzky et al., 2010). In our study, we show that the monoclonal TPPP/p25 antibody specifically detects mature OG in grey and white matter of nondiseased individuals as well as activated and degenerating/apoptotic OG in PPWM and plaques of demyelinated MS lesions but does not label astrocytes,

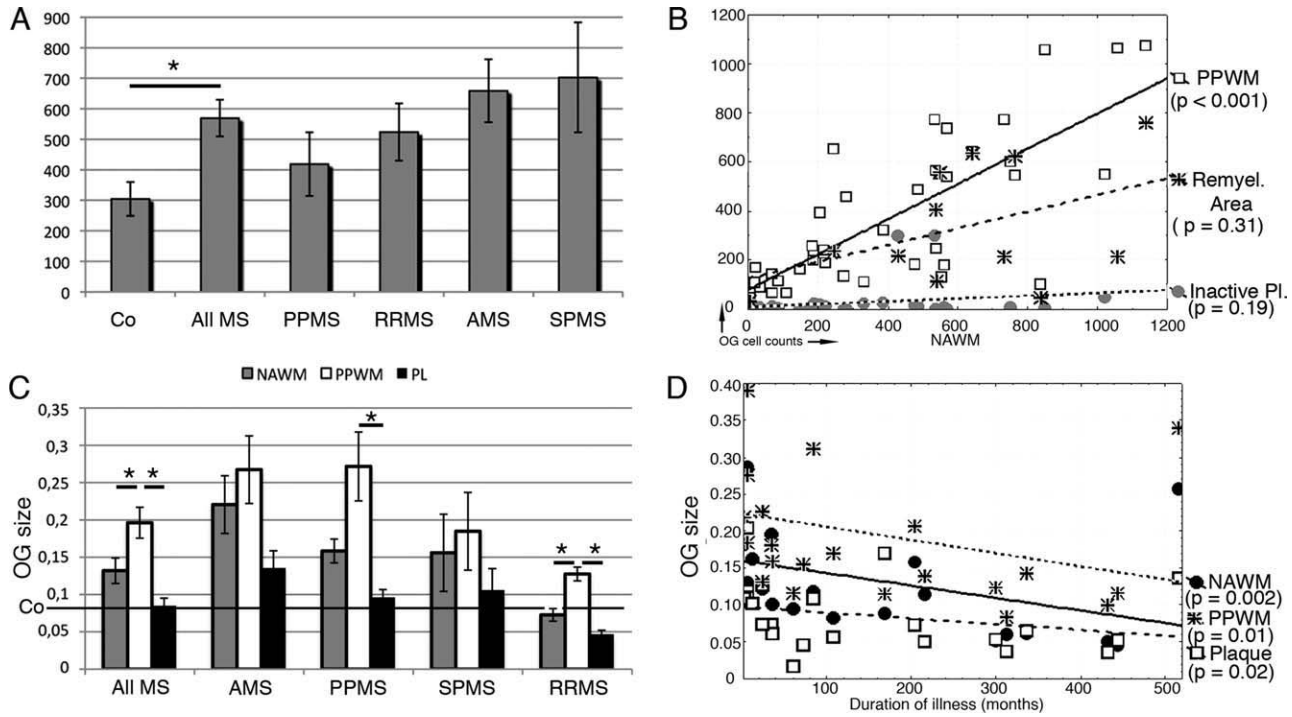

Fig. 4. Increased number and size of TPPP/p25 immunoreactive OG in MS patients. **A**: Bar graph representation of oligodendrocyte (OG) counts in controls (Co), multiple sclerosis (MS, pooled cases), primary progressive MS (PPMS), relapsing-remitting MS (RRMS), acute MS (AMS), and secondary progressive MS (SPMS). Significant difference is indicated with an asterisk. **B**: Scatter plot representation of OG counts in the normal appearing white matter (NAWM; x axis) versus periplaque WM (PPWM; y axis), remyelinating area (y axis), and inactive plaque (Pl; y axis) demonstrates a positive correlation between the OG counts in the NAWM and PPWM. **C**: Bar graph representation of TPPP/p25 immunoreactive OG cytoplasmic area in NAWM, PPWM, and plaque compared within all MS cases (pooled) and in each MS subtype. Mean value of OG cytoplasmic area in NWM in controls is indicated by a black line. Significant differences are indicated with an asterisk. **D**: Scatter plot representation of the correlation between TPPP/p25 immunoreactive OG cytoplasmic area in the NAWM (indicated by black dots), PPWM (indicated by stars), plaque (indicated by white boxes), and the duration of illness (x axis). Note that the highest values are consistently for PPWM.

microglia, or neurons. The number of TPPP/p25-positive OG in NWM of controls appears to be lower as described for OG labeled with other markers (Kuhlmann et al., 2009; Kuhlmann et al., 2008; Kuhlmann et al., 2007). This might be explained by the different brain regions evaluated in our study (periventricular region) when compared with other studies, or TPPP/p25-positive OG represent only a subset of mature OG. Clarification of what altered TPPP/p25 immunoreactive OG represent is hindered by the relative paucity of available antibodies for comparison that work on paraffin-embedded human brain tissue. Despite the presence of immunopositive cells throughout the brain, we detected qualitative and quantitative alterations of TPPP/p25 immunoreactive OG in WM of MS brains, and further studies are needed to define whether this reflects affection of all or only of a subset of OG.

In this study, we found higher numbers and increased size of TPPP/p25 positive OG in the NAWM and PPWM of MS compared with controls, which might suggest stimulatory effects on OG. However, with increasing age or longer disease duration, the numbers of TPPP/p25 positive OG were reduced. The loss of OG *per se*, or some components of the inflammatory milieu produced by macrophages or lymphocytes, might recruit mature OG from a pool of OPC, which might proliferate and migrate to demyelinating lesions and ensure remyelination (Di Bello et al., 1999; Keirstead et al., 1998). MS patients with significantly higher age and longer disease duration mainly showed late stage chronic inactive demyelinated lesions in our study and revealed lower numbers and smaller size of TPPP/p25 positive OG. This might reflect the absent, steadily ongoing, or even weaker inflammatory stimulation of OPC/OG, proliferation and maturation in chronic inactive lesions, or the higher age of these MS patients (Wolswijk, 2000). Alternatively, an impaired differentiation into mature OG in later disease stages due to a differentiation block of OPC might be discussed (Kuhlmann et al., 2008). Although our observations demonstrated clear differences between number and size of OG in MS and controls, our sample was not sufficiently large and representative to reach a conclusion regarding potential differences in OG changes between RRMS and progressive MS types.

TPPP/p25 specifically labels degenerating OG in the neurodegenerative disease MSA (Kovacs et al., 2007; Lindersson et al., 2005). It was suggested that during disease, TPPP/p25 (or also called p25α) relocalizes in OG from myelin as a sequence of events leading then to deposition and fibrillization of α-synuclein (Song et al.,

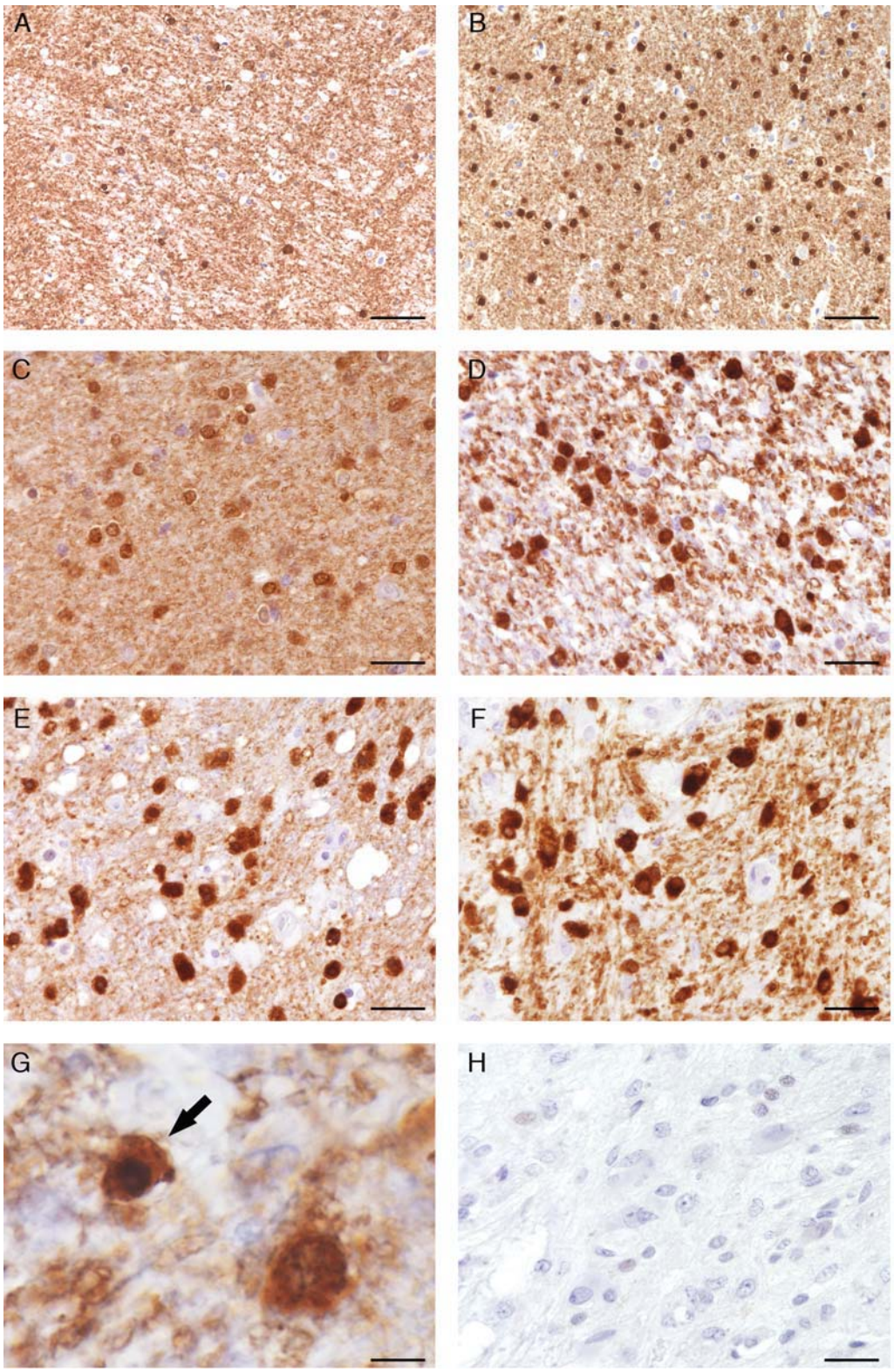

Fig. 5. Immunostaining for TPPP/p25 in MS and controls. TPPP/p25 immunoreactivity in a representative control (**A**) and MS case (**B**) reveals increased numbers of stained cells in MS. Comparison of NAWM (**C, E**) and PPWM (**D, F**) shows increased cytoplasmic immunoreactivity in the PPWM both in inactive (C, D) and active (E, F) lesions. Note TPPP/p25 immunoreactivity of apoptotic OG (**G**, arrow) and the lack of α-synuclein immunoreactivity in OG with enlarged cytoplasm (**H**). Bars: A, B: 70 μm, C-F, H: 35 μm, and G: 5 μm. [Color figure can be viewed in the online issue, which is available at wileyonlinelibrary.com.]

2007). Abnormal phosphorylation of microtubular proteins of the cytoskeleton are discussed to lead to glial cytoplasmic inclusions in MSA (Nakamura et al., 1998), with subsequent glial degeneration and secondary affection of neurons (Wenning et al., 1994; Wenning et al., 2008). MS is a heterogeneous disease with primary oligodendrogliopathy as one of four different pathogenetic patterns of demyelination (Lassmann et al., 2007). Indeed, one case of MS with numerous apoptotic OG, revealed some dense and globular TPPP/p25 immunoreactivity, suggesting early degenerative changes. Moreover, the apoptotic OG were strongly labeled. Despite the enlargement of OG cytoplasms, none of the MS cases investigated showed inclusion bodies comparable with those visible in MSA, as examined by α-synuclein immunohistochemistry and Gallyas staining. This might also indicate that the microtubular system in the cytoskeleton of OG is not primarily affected in MS. Indeed, in contrast with MS, the pathological neuronal inclusions of MSA are also TPPP/p25 immunoreactive. In our study, we did not observe any kind of neuronal expression of TPPP/p25. These observations suggest that the oligodendroglial reaction, as reflected by the altered TPPP/p25 immunostaining pattern, differs in distinct forms of MS from the primary neurodegenerative oligodendrogliopathy in MSA. Furthermore, this might also indicate that the pathogenesis of neuronal (and axonal) dysfunction may differ between MS and neurodegenerative diseases. An alternative pathogenetic mechanism discussed in MSA is an abnormal accumulation of α-synuclein with cytotoxic effects leading to cell death (Xu et al., 2002; Zhou et al., 2002). We could not find any α-synuclein immunopositive filamentous inclusions. However, some diffuse cytoplasmic staining, with variable amounts of positively labeled astrocytes, microglia, OG, and axons mainly in the PPWM and lesion edge were visible. A diffuse cytoplasmic upregulation of α-synuclein in neurons and glia in inflammatory demyelinating disease has been described (Lu et al., 2009). Whether this upregulation suggests a role for α-synuclein in neurodegenerative processes in MS or it reflects more a bystander effect, merits further studies. We could not find any immunoreactivity with antibodies tau AT-8, 3R-tau, and 4R-tau in axons or OG of demyelinated MS lesions. Interestingly, recent studies detected an accumulation of hyperphosphorylated tau in axons and spheroids, suggesting that abnormally phosphorylated tau plays a role in evolution of neuronal and axonal loss in MS (Anderson et al., 2008; Anderson et al., 2009). These investigations were performed on frozen tissue in contrast to the formalin-fixed and paraffin-embedded tissue in our study. However, the accumulation of insoluble tau in axons was not associated with the ultrastructural formation of tau filaments (Anderson et al., 2008). The sensitivity for the detection of hyperphosphorylated tau without fibril formation might be reduced in paraffin embedded compared with frozen tissue, possibly due to autolysis or embedding procedure, and could explain why we did not detect any immunoreactivity in axons within demyelinating MS lesions. Finally, we could not find any filamentous inclusions with the Gallyas stain or with antibody for TDP43, phospho-TDP-43, and p62 in OG or other cell types in MS lesions, suggesting that these proteins are not involved in the pathology of MS. Our observation might indicate that cytoplasmic accumulation of TPPP/p25 is a reactive process of the OG, however, due to yet unknown factors, including difference in the time course or the initiator genetic or epigenetic events, this does not lead to histologically detectable inclusion body formation in MS (e.g., in the lesion associated with primary oligodendrogliopathy) contrasting MSA.

In conclusion, we established a new monoclonal antibody directed against TPPP/p25, which was found highly specific for OG and myelin. Our data provide the first systematic quantification of TPPP/p25-positive mature OG in different lesion types in MS. Since number and size of TPPP/p25-positive OG were significantly increased in MS, TPPP/p25 might serve as potential prognostic and diagnostic marker in MS.

ACKNOWLEDGMENTS

The authors thank Irene Leisser and Judith Ludwig for expert technical assistance.

REFERENCES

Anderson JM, Hampton DW, Patani R, Pryce G, Crowther RA, Reynolds R, Franklin RJ, Giovannoni G, Compston DA, Baker D, Spillantini MG, Chandran S. 2008. Abnormally phosphorylated tau is associated with neuronal and axonal loss in experimental autoimmune encephalomyelitis and multiple sclerosis. Brain 131:1736–1748.

Anderson JM, Patani R, Reynolds R, Nicholas R, Compston A, Spillantini MG, Chandran S. 2009. Evidence for abnormal tau phosphorylation in early aggressive multiple sclerosis. Acta Neuropathol 117: 583–589.

Baumann N, Pham-Dinh D. 2001. Biology of oligodendrocyte and myelin in the mammalian central nervous system. Physiol Rev 81:871–927.

Blakemore WF. 1974. Pattern of remyelination in the CNS. Nature 249: 577–578.

Bradford MM. 1976. A rapid and sensitive method for the quantitation of microgram quantities of protein utilizing the principle of protein-dye binding. Anal Biochem 72:248–254.

Bruck W, Porada P, Poser S, Rieckmann P, Hanefeld F, Kretzschmar HA, Lassmann H. 1995. Monocyte/macrophage differentiation in early multiple sclerosis lesions. Ann Neurol 38:788–796.

Cahoy JD, Emery B, Kaushal A, Foo LC, Zamanian JL, Christopherson KS, Xing Y, Lubischer JL, Krieg PA, Krupenko SA, Thompson WJ, Barres BA. 2008. A transcriptome database for astrocytes, neurons, and oligodendrocytes: A new resource for understanding brain development and function. J Neurosci 28:264–278.

Chang A, Tourtellotte WW, Rudick R, Trapp BD. 2002. Premyelinating oligodendrocytes in chronic lesions of multiple sclerosis. N Engl J Med 346:165–173.

Di Bello IC, Dawson MR, Levine JM, Reynolds R. 1999. Generation of oligodendroglial progenitors in acute inflammatory demyelinating lesions of the rat brain stem is associated with demyelination rather than inflammation. J Neurocytol 28:365–381.

Dubois-Dalcq M, Williams A, Stadelmann C, Stankoff B, Zalc B, Lubetzki C. 2008. From fish to man: Understanding endogenous remyelination in central nervous system demyelinating diseases. Brain 131:1686–1700.

Goldschmidt T, Antel J, Konig FB, Bruck W, Kuhlmann T. 2009. Remyelination capacity of the MS brain decreases with disease chronicity. Neurology 72:1914–1921.

Hlavanda E, Kovacs J, Olah J, Orosz F, Medzihradszky KF, Ovadi J. 2002. Brain-specific p25 protein binds to tubulin and microtubules and induces aberrant microtubule assemblies at substoichiometric concentrations. Biochemistry 41:8657–8664.

Hoftberger R, Aboul-Enein F, Brueck W, Lucchinetti C, Rodriguez M, Schmidbauer M, Jellinger K, Lassmann H. 2004. Expression of major histocompatibility complex class I molecules on the different cell types in multiple sclerosis lesions. Brain Pathol 14:43–50.

Hoftberger R, Kunze M, Weinhofer I, Aboul-Enein F, Voigtlander T, Oezen I, Amann G, Bernheimer H, Budka H, Berger J. 2007. Distribution and cellular localization of adrenoleukodystrophy protein in human tissues: Implications for X-linked adrenoleukodystrophy. Neurobiol Dis 28:165–174.

Keirstead HS, Levine JM, Blakemore WF. 1998. Response of the oligodendrocyte progenitor cell population (defined by NG2 labelling) to demyelination of the adult spinal cord. Glia 22:161–170.

Kohler G, Milstein C. 1975. Continuous cultures of fused cells secreting antibody of predefined specificity. Nature 256:495–497.

Kovacs GG, Gelpi E, Lehotzky A, Hoftberger R, Erdei A, Budka H, Ovadi J. 2007. The brain-specific protein TPPP/p25 in pathological protein deposits of neurodegenerative diseases. Acta Neuropathol 113:153–161.

Kovacs GG, Laszlo L, Kovacs J, Jensen PH, Lindersson E, Botond G, Molnar T, Perczel A, Hudecz F, Mezo G, Erdei A, Tirián L, Lehotzky A, Gelpi E, Budka H, Ovádi J. 2004. Natively unfolded tubulin polymerization promoting protein TPPP/p25 is a common marker of alpha-synucleinopathies. Neurobiol Dis 17:155–162.

Kuhlmann T, Goldschmidt T, Antel J, Wegner C, Konig F, Metz I, Bruck W. 2009. Gender differences in the histopathology of MS? J Neurol Sci 286:86–91.

Kuhlmann T, Miron V, Cuo Q, Wegner C, Antel J, Bruck W. 2008. Differentiation block of oligodendroglial progenitor cells as a cause for remyelination failure in chronic multiple sclerosis. Brain 131:1749–1758.

Kuhlmann T, Remington L, Maruschak B, Owens T, Bruck W. 2007. Nogo-A is a reliable oligodendroglial marker in adult human and mouse CNS and in demyelinated lesions. J Neuropathol Exp Neurol 66:238–246.

Lassmann H, Bruck W, Lucchinetti CF. 2007. The immunopathology of multiple sclerosis: An overview. Brain Pathol 17:210–218.

Lehotzky A, Lau P, Tokesi N, Muja N, Hudson LD, Ovadi J. 2010. Tubulin polymerization-promoting protein (TPPP/p25) is critical for oligodendrocyte differentiation. Glia 58:157–168.

Lehotzky A, Tirian L, Tokesi N, Lenart P, Szabo B, Kovacs J, Ovadi J. 2004. Dynamic targeting of microtubules by TPPP/p25 affects cell survival. J Cell Sci 117:6249–6259.

Lindersson E, Lundvig D, Petersen C, Madsen P, Nyengaard JR, Hojrup P, Moos T, Otzen D, Gai WP, Blumbergs PC, Jensen PH. 2005. p25alpha Stimulates alpha-synuclein aggregation and is colocalized with aggregated alpha-synuclein in alpha-synucleinopathies. J Biol Chem 280:5703–5715.

Lindner M, Heine S, Haastert K, Garde N, Fokuhl J, Linsmeier F, Grothe C, Baumgartner W, Stangel M. 2008. Sequential myelin protein expression during remyelination reveals fast and efficient repair after central nervous system demyelination. Neuropathol Appl Neurobiol 34:105–114.

Lu JQ, Fan Y, Mitha AP, Bell R, Metz L, Moore GR, Yong VW. 2009. Association of alpha-synuclein immunoreactivity with inflammatory activity in multiple sclerosis lesions. J Neuropathol Exp Neurol 68:179–189.

McDonald WI, Compston A, Edan G, Goodkin D, Hartung HP, Lublin FD, McFarland HF, Paty DW, Polman CH, Reingold SC, Sandberg-Wollheim M, Sibley W, Thompson A, van den Noort S, Weinshenker BY, Wolinsky JS. 2001. Recommended diagnostic criteria for multiple sclerosis: Guidelines from the International Panel on the diagnosis of multiple sclerosis. Ann Neurol 50:121–127.

Nakamura S, Kawamoto Y, Nakano S, Akiguchi I, Kimura J. 1998. Cyclin-dependent kinase 5 and mitogen-activated protein kinase in glial cytoplasmic inclusions in multiple system atrophy. J Neuropathol Exp Neurol 57:690–698.

Olah J, Tokesi N, Vincze O, Horvath I, Lehotzky A, Erdei A, Szajli E, Medzihradszky KF, Orosz F, Kovacs GG, Ovádi J. 2006. Interaction of TPPP/p25 protein with glyceraldehyde-3-phosphate dehydrogenase and their co-localization in Lewy bodies. FEBS Lett 580:5807–5814.

Patrikios P, Stadelmann C, Kutzelnigg A, Rauschka H, Schmidbauer M, Laursen H, Sorensen PS, Bruck W, Lucchinetti C, Lassmann H. 2006. Remyelination is extensive in a subset of multiple sclerosis patients. Brain 129:3165–3172.

Prineas JW, Barnard RO, Kwon EE, Sharer LR, Cho ES. 1993. Multiple sclerosis: Remyelination of nascent lesions. Ann Neurol 33:137–151.

Prineas JW, Kwon EE, Goldenberg PZ, Ilyas AA, Quarles RH, Benjamins JA, Sprinkle TJ. 1989. Multiple sclerosis. Oligodendrocyte proliferation and differentiation in fresh lesions. Lab Invest 61:489–503.

Raine CS, Wu E. 1993. Multiple sclerosis: Remyelination in acute lesions. J Neuropathol Exp Neurol 52:199–204.

Skjoerringe T, Lundvig DM, Jensen PH, Moos T. 2006. P25alpha/Tubulin polymerization promoting protein expression by myelinating oligodendrocytes of the developing rat brain. J Neurochem 99:333–342.

Song YJ, Lundvig DM, Huang Y, Gai WP, Blumbergs PC, Hojrup P, Otzen D, Halliday GM, Jensen PH. 2007. p25alpha relocalizes in oligodendroglia from myelin to cytoplasmic inclusions in multiple system atrophy. Am J Pathol 171:1291–1303.

Wenning GK, Quinn N, Magalhaes M, Mathias C, Daniel SE. 1994. "Minimal change" multiple system atrophy. Mov Disord 9:161–166.

Wenning GK, Stefanova N, Jellinger KA, Poewe W, Schlossmacher MG. 2008. Multiple system atrophy: A primary oligodendrogliopathy. Ann Neurol 64:239–246.

Wolswijk G. 2000. Oligodendrocyte survival, loss and birth in lesions of chronic-stage multiple sclerosis. Brain 123:105–115.

Xu J, Kao SY, Lee FJ, Song W, Jin LW, Yankner BA. 2002. Dopamine-dependent neurotoxicity of alpha-synuclein: A mechanism for selective neurodegeneration in Parkinson disease. Nat Med 8:600–606.

Zhou W, Schaack J, Zawada WM, Freed CR. 2002. Overexpression of human alpha-synuclein causes dopamine neuron death in primary human mesencephalic culture. Brain Res 926:42–50.